Work Term 2 - COOP Report

Ivan Zhenchuk

Kaon Beam Spin Asymmetry Study

Student #: 200482575

Employer: Dr. G. M. Huber, Department of Physics, University of Regina, Regina, SK

September 5, 2025

Contents

1 Executive Summary

The experimental Hall C at Jefferson Lab focuses on studying the internal structure of protons. Hall C uses the electrons accelerated in Jefferson Lab's accelerator to probe the proton. With energies up to 12 GeV, Hall C studies the changes in electron-proton interaction cross sections at different energies. This study of Kaon beam spin asymmetry investigates one of energy settings to measure the interference cross section of longitudinally and transversely polarized virtual photons that transmit energy between an electron and a proton. The study looks at the Kaon production channel for asymmetry between positive and negative helicity electrons.

The data is collected by coincidence method between two movable magnetic spectrometers. This method allows the identification of neutral (undetected) baryon via the missing mass method. Λ^0 baryon is the baryon produced alongside the K^+ meson in Kaon production channel of electron-proton interaction. After background filtering and particle identification, the yield of Λ^0 from different helicities are compared and the interference cross section is extracted.

The results of this study show that the interference cross section does have a non-zero value with increase of K^+ fraction of energy. Although the systematic errors were not yet applied, the results are not expected to change. The next step of this study is to finalize the systematic errors and prepare the full results.

2 Introduction

Probing the insides of particles like proton requires us to break it, and then study the resulting products. This is a typical method used by physicists. This study looks at products of a proton (valence quark contents:uud) that is hit by an accelerated electron. The products that this study is interested in are K^+ meson ($u\bar{s}$) and Λ^0 baryon (uds). The strange/anti-strange quark pair appears from the sea quarks of the proton. The sea quarks are normally inaccessible to view but they do give proton a fraction of its mass (0.938 GeV/c^2 is the full mass). Due to quark/anti-quark pairs in the sea region, the major properties of sea quarks are masked, but they rise up when enough energy is supplied to break the proton apart.

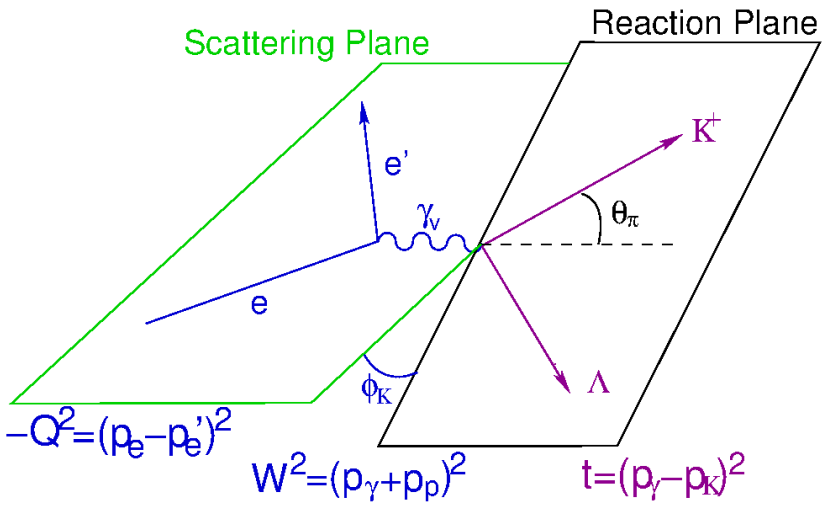

Figure 1: An image demonstrating the deep exclusive meson production (DEMP). In this case, the reaction produces a K^+ meson and a Λ baryon. The three primary kinematic variables are also shown. Q^2 is the electron 4-momentum transfer. W is the invariant mass of the system. t is the fraction of 4-momentum passed to K^+. Figure is from [1]

The electron that reacts with the proton (ep) transfers its 4-momentum via a virtual photon. The 4-momentum is a four dimensional property that included three momentum dimensions and one energy dimension. 4-momentum is useful to simplify conservation

laws calculations in relativistic collisions. When the virtual photon breaks the proton, the 4-momentum is divided between two product particles, K^+ meson (Kaon) and a Λ^0 baryon (Λ). The cross section of this interaction (strange quark release) is studied by looking at produced Kaons and Λs.

The cross section is studied by varying the initial conditions of the reaction and observing final results. However, the cross section is broken into multiple parts due to polarization of the virtual photon. Unlike real photons with transverse polarization, virtual photons can have transverse (T), longitudinal (L), and combined (LT) polarization. In this study, the helicity of incoming electron is used to study the interference (LT) cross sections of the reaction. The helicity is the direction of the spin relative to particles momentum direction. Parallel spin and momentum give positive helicity and anti-parallel spin and momentum gives negative helicity. It is expected that the helicity value changes the yields of Λ and Kaons.

Measurement of beam spin asymmetry (BSA) is used for calculating the interference cross section of (ep) reaction. Measuring BSA is done by comparing the yield of produced particles with positive and negative helicities. The relative difference in yields of positive and negative helicity particles gives the BSA value.

$$BSA = \frac{1}{P}\frac{Y^+ - Y^-}{Y^+ + Y^-} \tag{1}$$

In equation 1, $Y^{+/-}$ are the positive and negative yield, and P is the polarization amount of the beam. A different form of the BSA equation comes from L/T separation of differential cross section. Equation 2a provides the values necessary for extracting interference term.

$$BSA = \frac{\sqrt{2\epsilon(1-\epsilon)}\frac{\sigma_{LT'}}{\sigma_0}sin(\phi)}{1+\sqrt{2\epsilon(1+\epsilon)}\frac{\sigma_{LT}}{\sigma_0}cos(\phi)+\epsilon\frac{\sigma_{TT}}{\sigma_0}cos(2\phi)} \tag{2a}$$

The form of equation 2a that is used in the experiment assumes the numerator to be 1 due to both cosine terms approaching 0. The experimental form of the equation is as follows:

$$BSA \approx A \cdot sin(\phi) \tag{2b}$$

In equation 2b, A is the parameter that holds the interference variable $\frac{\sigma_{LT'}}{\sigma_0}$. The $\frac{\sigma_{LT'}}{\sigma_0}$ term is the interference cross section. The cross section can give insights into the L/T separation parameters when compared to kinematic variables of the particle collision.

The kinematic variables Q^2 and W are the primary kinematic variables of the reaction defined in figure 1. These experimentally controlled variables create a setting for the experiment. This study focuses on a setting where $Q^2 = 0.5GeV^2$ and $W = 2.40GeV$. The variable t (also defined in Fig. 1) is used to study the behavior of $\frac{\sigma_{LT'}}{\sigma_0}$ and presence of asymmetry with changing momentum of K^+. The angle between the scattering and reaction plane ϕ is captured for a 360° range. The BSA has a trend over angle ϕ as shown in equation 2b. The final kinematic variable used in this study is ϵ, which is the ratio between longitudinal and transverse virtual photon yields. ϵ can be experimentally controlled and set to a high or low setting. The data for this study is high ϵ.

3 Experimental Setup

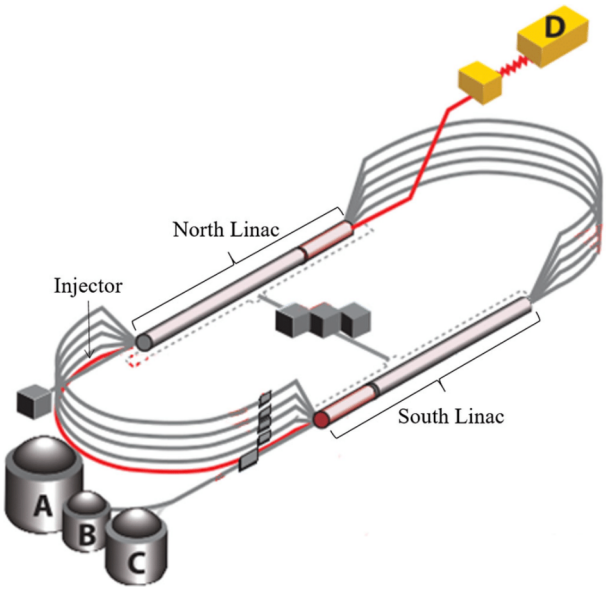

Figure 2: Accelerator facility scheme for Jefferson Lab. This accelerator delivers a continuous electron beam to all four halls simultaneously, with energies up to 12 GeV. Hall C is the facility from which the data is collected for this study uses. Figure from [3]

The Kaon-LT experiment is conducted in Hall C of Thomas Jefferson National Accelerator Facility, or JLab. JLab uses Continuous Electron Beam Accelerator Facility (CEBAF) as its accelerator. CEBAF uses 2 linear accelerators along with five loops to produce energies up to 12 GeV. The continuous electron beam is distributed to four halls. Hall C facility is used to study hadron structure. Hall C houses two detectors and the target stack for the electron beam.

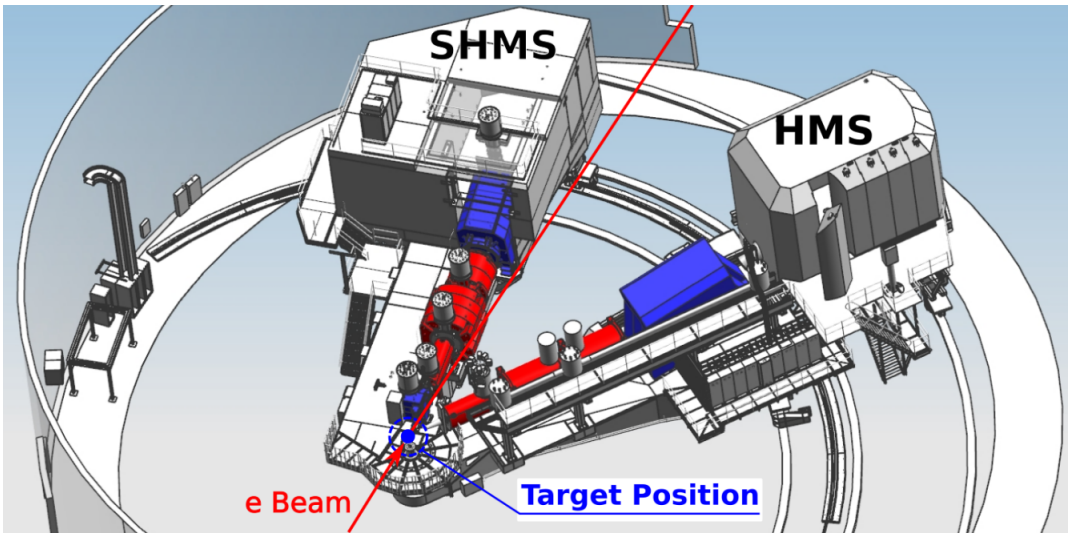

Figure 3: Hall C aerial CAD rendering. Two movable magnetic spectrometers are used for particle detection. The spectrometers are high resolution but low acceptance. This feature requires the spectrometers to be moved by rails to collect all angles of the reaction. Figure from [2]

Super High Momentum Spectrometer (SHMS) is the hadron detector of Hall C. After the electron beam hits the target, a set of superconducting magnets directs and focuses the produced particles into SHMS detector stack. The magnets consist of five magnets. One dipole magnet at the beginning to direct particles into focusing plane. Three quadrupole magnets focus the incident particles. Last dipole magnet directs positive particles into the detector stack. [4]

The stack consists of noble and heavy gas cherenkovs, 4 hodoscopes, 2 drift chambers, an aerogel cherenkov, and a lead glass shower calorimeter. The magnets create a beam of uniform momentum dispersion that is filtered with acceptance cuts to provide set momentum with slight variation. This final beam is then filtered further by particle identification (PID) cuts and coincidence with electron from HMS.

The cherenkov detectors provide an efficient way to apply PID cuts on SHMS. The cherenkov detector's material determines its index of refraction and with that, which

particle will create cherenkov radiation. The Argon/Neon cherenkov has the lowest index of refraction (n=1.00028201/=1.000066102) allowing only electrons and positrons to cherenkov.[4] The heavy gas cherenkov has a medium index of refraction (n=1.00143) which, in addition, allows π^+ and some fast kaons to cherenkov. The aerogel cherenkov has the highest indices of refraction (n=1.030, 1.020, 1.015, 1.011) with physical options to swap for different energies.

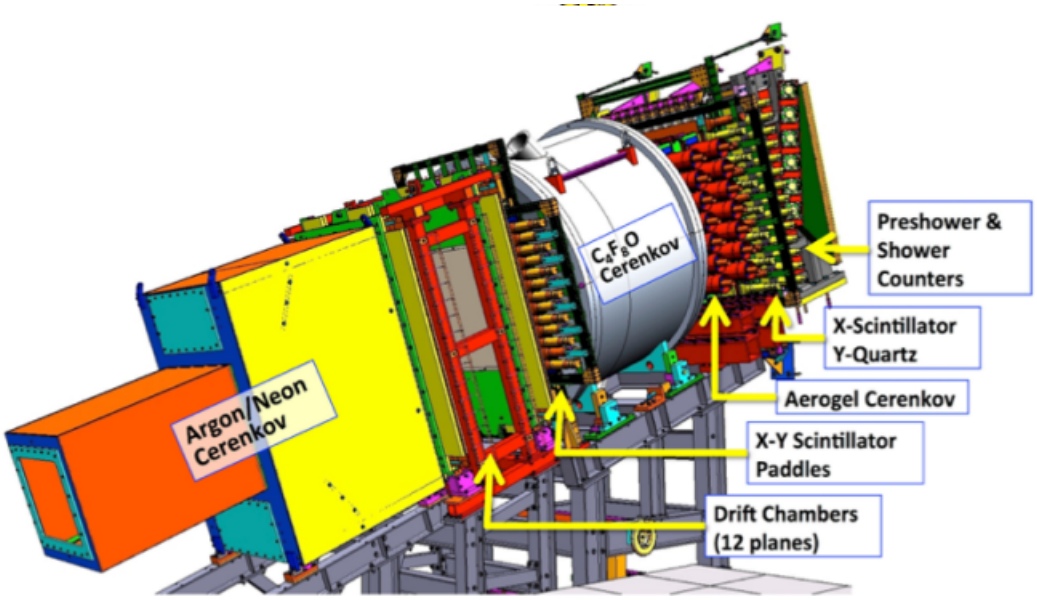

Figure 4: Super High Momentum spectrometer detector stack CAD rendering. The baryons produced in the target chamber are directed into this detector stack by a set of quadrupole and dipole magnets. SHMS is upgraded HMS that was designed to accept up to 12 GeV particles. Figure from [2]

High Momentum Spectrometer (HMS) is the electron detector that is used for determining coincidence time between hadron and electron pair. Like the SHMS, HMS contains superconducting magnets that focus particles into the viewing plane of detector stack. Three quadrupole magnets focus the incident electron and only one dipole bends it into the detector housing. HMS detector stack consists of a pair of drift chambers, 2 pairs of scintillator hodoscopes, a gas cherenkov, and a lead glass shower calorimeter.

$$t_{coin}(ns) = t_{HMS} \ - \ t_{SHMS} \tag{3}$$

Main use of HMS is to measure the coincidence time between the electron and the target hadron. Coincidence time method involves measuring the produced meson and recoiled electron simultaneously to make sure the particles come from the same interaction. Equation 3 shows the coincidence equation in nanoseconds. Coincidence method allows for accurate reconstruction of reactions. In Kaon DEMP reaction, accurate reconstruction is necessary to detect the Λ baryon produced. Λ is not directly detected; it is inferred from the missing mass after reaction reconstruction. Equation 4 shows missing mass as equation derived from 4 momenta for Λ baryon as a missing particle.

$$p_{\Lambda}^2 = (p_e + p_p - p_{e'} - p_{K^+})^2 = m_{miss}^2 \tag{4}$$

HMS also undergoes the acceptance filtering to ensure certain range of momenta enters the detector stack. For electron selection HMS uses the heavy gas cherenkov counts and track normalized calorimeter counts. The calorimeter selects the electrons based on energy deposition and heavy gas cherenkov filters out some background light particles.

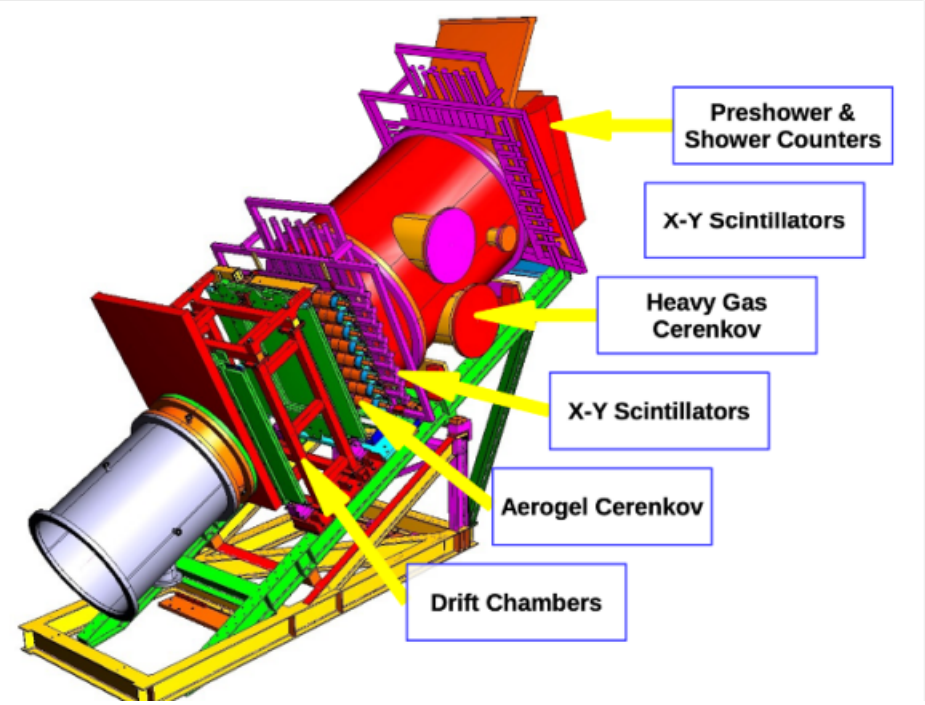

Figure 5: High Momentum Spectrometer detector stack CAD rendering. Electrons are directed here using multiple quadrupole magnets and a dipole magnet. HMS is the legacy detector that is used for coincidence measurement. Figure from [2]

4 Analysis

To analyze the behavior of $\frac{\sigma_{LT'}}{\sigma_0}$ with relation to t, a BSA has to be analyzed with relation to ϕ (Defined in Fig. 1). To calculate BSA for this study, a clean sample of Kaon Λ has to be selected. This selection process makes up the bulk of the analysis done. A number of histogram cuts are applied to separate different particles and random backgrounds. The unwanted data is then removed from main sample with histogram subtractions to produce a clean sample of Kaon missing mass (MMK) histogram. MMK histogram provides distributions for undetected baryons produced in Kaon DEMP. The Λ distribution is selected to provide the kaon yield for this study.

To ensure the kaon sample is free from other radiation sources and all particles in

detectors come from the same reaction, a coincidence method is used. This allows for partial PID based on CTime. CTime also differentiates between the background events and the prompt peak of interest. The CTime counts belonging to random events are used to select a random sample which is then subtracted from the prompt peak. This cleans up a bulk of events in the MMK histogram.

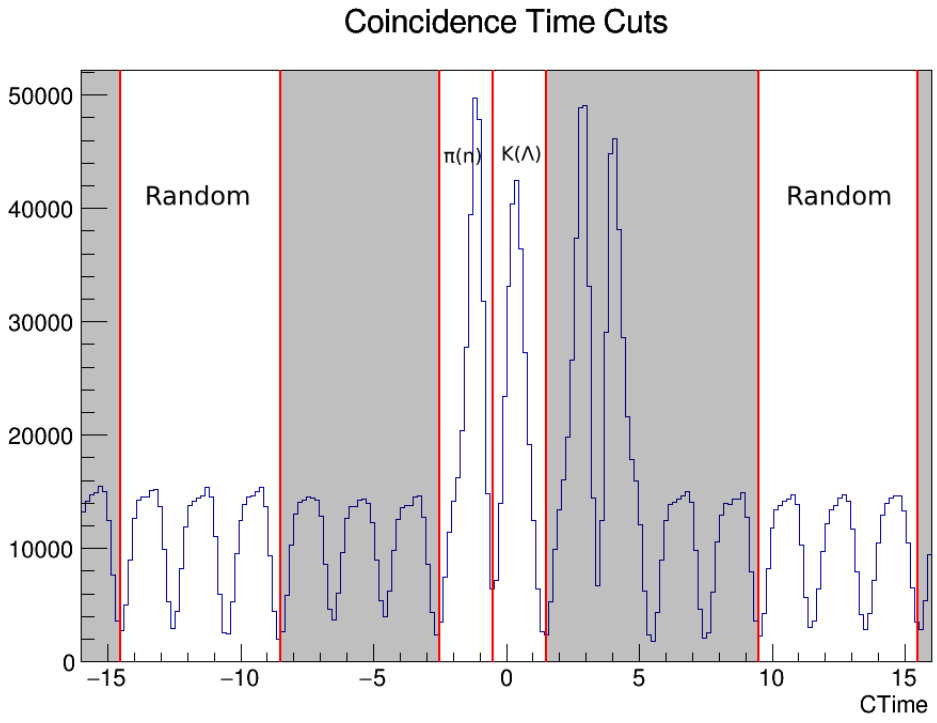

Figure 6: Coin Time histogram with Kaon PID and Kaon PID and MMK cuts. Peaks beside the K(Λ) are the particles leaking into Kaon sample. Gray area particles and $\pi(n)$ are excluded with CTime cuts. Random areas are used to subtract a random background sample from Pions and Kaon samples.

SHMS does not only detect Kaon, but also all other possible channels from electron proton scattering. Specific PID cuts are used to further separate the Kaons, Pions, and other particles. Although heavy gas and aerogel cherenkovs in SHMS can be used for PID purpose, in this study Radio Frequency (RF) distribution separation was the preferred method for PID. Heavy gas has an inefficiency region (heavy gas hole) that creates a

Kaon leak into a Pion sample. The leaks results in over subtraction of Pions from Kaons. RF uses the difference time when the electron pulse hits the target and when produced particle is registered in SHMS. Due to momentum and distance of flight being known, particle mass can be calculated and separated in RF histogram.

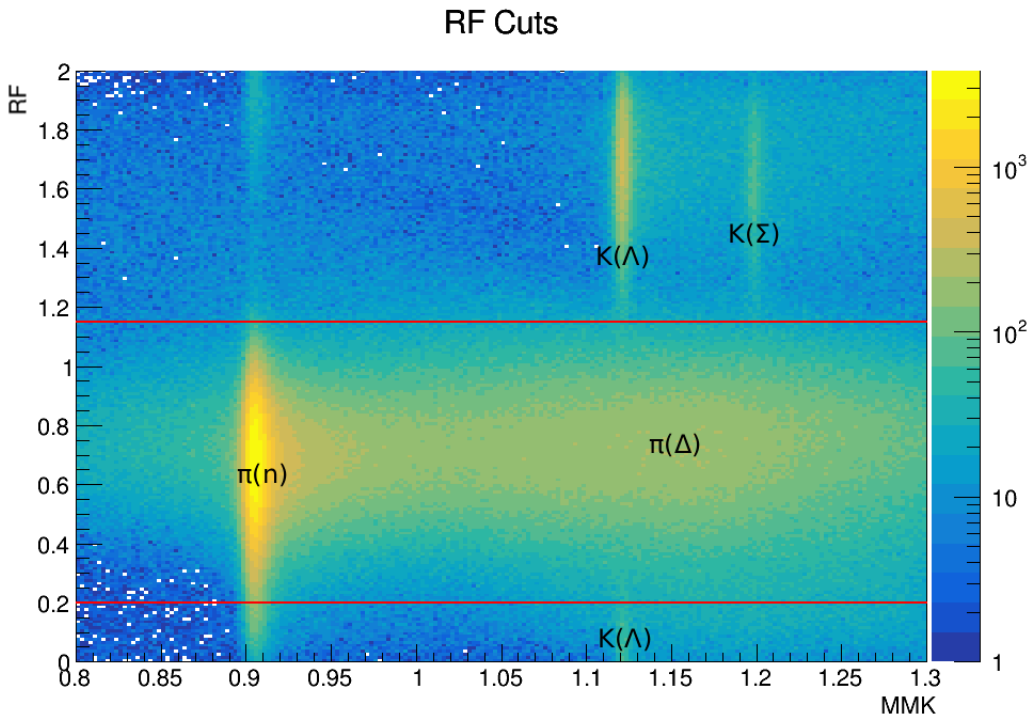

Figure 7: RF vs MMK histogram. Different particles are labeled. Red lines separate the Kaons from Pion. There is some leak through of particles into one another. The subtraction of samples removes majority of unwanted particles.

Variables cuts applied to kaon sample

Variable	Low	High
H.cer.npeSum	2	-
H.cal.etottracknorm	0.5	-
CTime.eKCoinTime_ROC1 (Kaon)	-0.5	1.5
RFTime.SHMS_RFtimeDist*(3.05*P.gtr.th)	1.2	0.2

Table 1: The cuts applied are used to select a kaon sample. HMS (H.) cuts are used for all

particles to select only electrons in HMS. RF used for cutting is corrected by central (golden track) momentum. Similar cuts are used to select other particles and events.

Even after the CTime and PID cuts, the Kaon sample has significant background events. Random data is the most significant part of Kaon's background. Pions and aluminum target housing are less pronounced sources of background but still contribute a significant amount to the Kaon sample. Each of these backgrounds are separately selected, scaled, and subtracted. Pions are scaled using an integral of Pion neutron region in Kaon and Pion samples. The scaling factor is constant and is selected with no t or ϕ bins (Variables defined in Fig. 1). The factor is manually adjusted depending on how well the subtraction performs with varying t an ϕ.

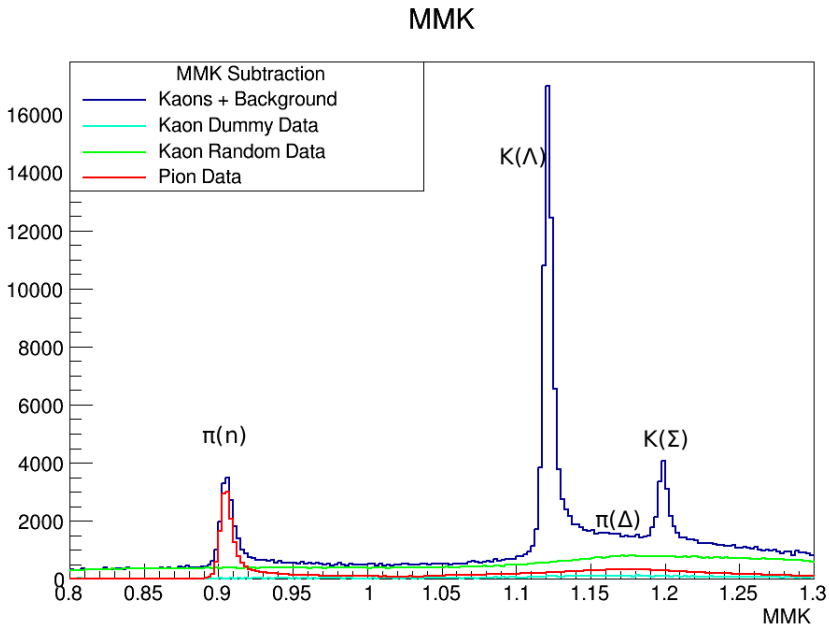

Figure 8: Kaon sample and the subtractions that are applied to it. The largest peak are K(Λ) and are the particles of interest. Pion data uses the $\pi(n)$ peak for scaling to the kaon sample after the kaon sample is free from dummy-shell target and random data.

After subtraction are applied to the MMK Kaon sample, Kaon Λ section ($1.080GeV <$ MMK $< 1.183GeV$) is selected for yield calculation. Integrating the Kaon Λ section with

the positive and negative helicity data gives us the Y^+ and Y^- for equation 1. This operation is performed for 15 bins in ϕ per each t bin. The plot of BSA vs ϕ (Figure 9) is used to extract A in equation 3. Parameter A is converted to $\frac{\sigma_{LT'}}{\sigma_0}$, by using the ϵ histogram that was cleaned and averaged for each t bin in the same way a Kaon MMK sample was cleaned.

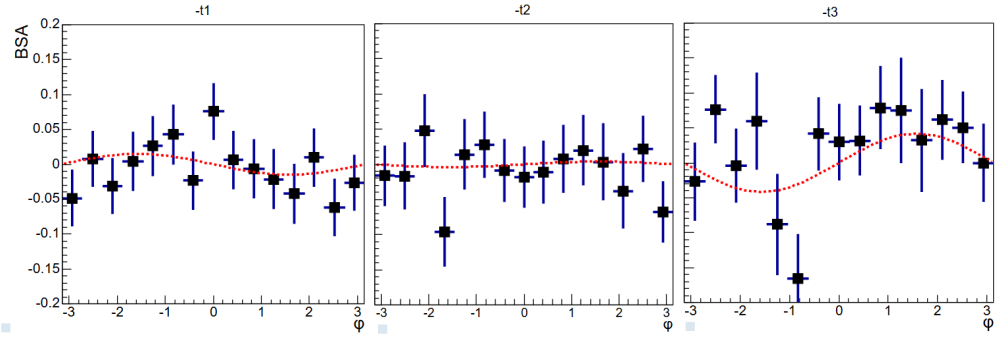

Figure 9: Three t bins of BSA vs ϕ plots. The fit is a simple $\sin(\phi)$ fit with one parameter A. Amplitude of the fit is proportional to the asymmetry and $\frac{\sigma_{LT'}}{\sigma_0}$ in the respective t bin.

5 Results

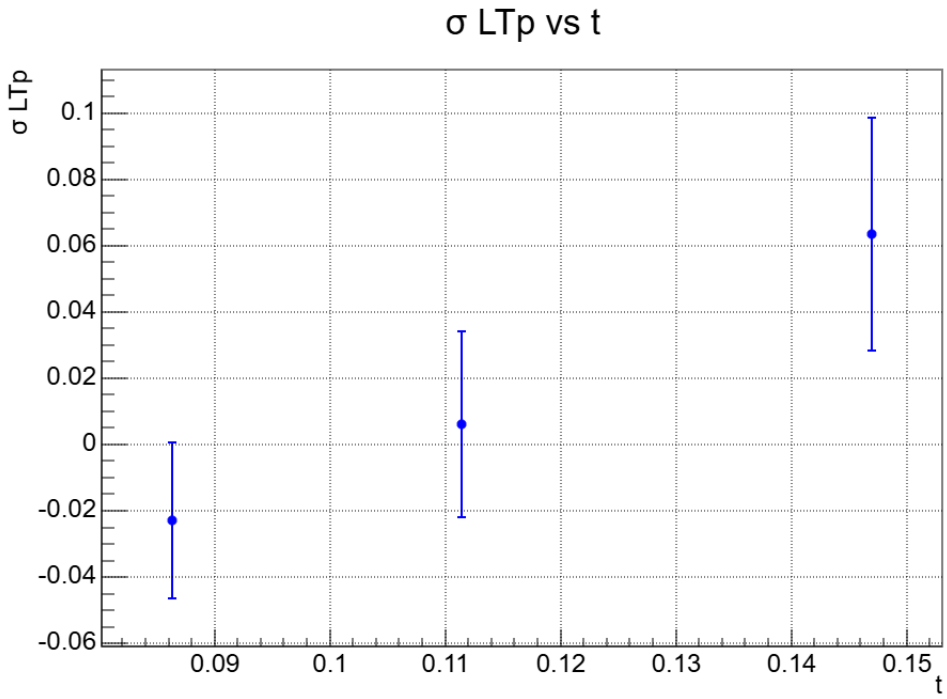

Figure 10: $\frac{\sigma_{LT'}}{\sigma_0}$ dependence on t. The first two points have no significant asymmetry. The third t bin provides evidence of some asymmetry, although very small. The error bars do not have systematic errors applied.

Kaon Λ has non-zero asymmetry at $Q^2 = 0.5GeV^2$ and $W = 2.40GeV$ experimental setting for high t. Although asymmetry is zero for the first two t bins, the high t asymmetry is statistically greater then zero. The error bars reflect statistical uncertainty only and do not have systematic uncertainty applied. The systematic errors observed so far do not significantly increase the total error (+0.11%).

6 Discussion and Conclusion

As seen in Figure 8, Kaon Λ are not the only Kaon DEMP products. The $Q^2 = 0.5GeV^2$ setting can also be used to find asymmetry in Kaon Σ and Pion neutron. In

fact, Pion neutron was analyzed as part of verifying the procedure of BSA calculation of Kaon Λ. While not the focus of the study, there was an observed small asymmetry for pions. The pion asymmetry is about 100 times smaller and is entirely negative compared to Kaon Λ Pions make up the bulk of the data resulting in very small statistical errors in their $\frac{\sigma_{LT'}}{\sigma_0}$. High statistics also allowed for more t bins. On the other hand, Kaon Σ had very poor statistics resulting in inconclusive asymmetry estimates. Very poor statistics made it unreasonable to expand the study's scope to Kaon Σ.

The promising results of $Q^2 = 0.5GeV^2$ setting prompted some investigation into higher Q^2. While the data was intended for pion research, enough Kaon statistics were observed to extract the asymmetry. The asymmetry of higher Q^2 was significantly greater compared to $Q^2 = 0.5GeV^2$. This check allows for extending the methods of this study to higher Q^2. The issues arise due to many cuts and selected regions do not stay constant when analyzing different setting.

The systematic error of this study are calculated, but are at the preliminary stages. The systematic errors include: PID cut values, yield integral area, Pion scaling factor, and CTime cut values. The systematic error analysis checked how much does variation in guided arbitrary selection affects the final results. Results from slightly varied variables were combined by root mean squared method. PID, HMS electron selection, CTime, and MMK yield integral boundaries had a the greatest contribution to the systematic error. The Pion scaling factor resulted in very small variation. The next steps of the study is to complete the systematic analysis.

The Kaon BSA study at low Q^2 fills data holes in energy region that is not popular place to study. With further refinement, this data can be used to guide further exploration and modeling of low energy cross sections. Likewise, methods used in this study can be applied to other particles present in low energy setting and kaons at higher energies. Finding a non-zero asymmetry is good, but more statistics can make it better.

7 Acknowledgments

Thanks to USRA and Garth Huber for sponsoring this project. Thanks to Alicia Postuma, Abdenacer Hamdi, Nathan Heinrich, Ali Usman, Muhammad Junaid and Vijay Kumar for assistance in learning and working.

References

[1] Usman, A. (2021, January 29). Update on Kaon-LT Experiment [PowerPoint slides]. Faculty of Physics, University of Regina. http://lichen.phys.uregina.ca/index_files/talks/usman_HallCmeeting_21jan.pdf

[2] Kinney, E.R. (2022, September 24). The Jefferson Lab Hall C Program: Physics at the Luminosity Frontier [PowerPoint slides]. University of Colorado. https://indico.mit.edu/event/538/contributions/1509/attachments/562/950/Kinney_HallC_v1%20Ed%20Kinney.pdf

[3] Tennant, Chris & Carpenter, Adam & Powers, Tom & Solopova, Anna & Vidyaratne, Lasitha & Iftekharuddin, Khan. (2020). Superconducting radio-frequency cavity fault classification using machine learning at Jefferson Laboratory. Physical Review Accelerators and Beams. 23. 10.1103/PhysRevAccelBeams.23.114601.

[4] S. Ali, A. Ahmidouch, G. R. Ambrose, A. Asaturyan, C. Ayerbe Gayoso, J. Benesch, V. Berdnikov, H. Bhatt, D. Bhetuwal, D. Biswas, P. Brindza, M. Bukhari, M. Burton, R. Carlini, M. Carmignotto, M. E. Christy, C. Cotton, J. Crafts, D. Day, S. Danagoulian, A. Dittmann, D. H. Dongwi, B. Duran, D. Dutta, R. Ent, H. Fenker, M. Fowler, D. Gaskell, A. Hamdi, N. Heinrich, W. Henry, N. Hlavin, T. Horn, G. M. Huber, Y. Ilieva, J. Jarrell, S. Jia, M. K. Jones, M. Junaid, M. L. Kabir, N. Kalantarians, A. Karki, S. J. D. Kay, C. E. Keppel, V. Kumar, S. Lassiter, W. B. Li,

D. Mack, S. Malace, J. McMahon, A. Mkrtchyan, H. Mkrtchyan, P. Monaghan, C. Morean, P. Nadel-Turonski, G. Niculescu, M. I. Niculescu, A. Nadeeshani, J. Pan, E Pooser, J. Okine, A. Ramos, J. Reinhold, B. Sawatzky, I. Steel, H. Szumila-Vance, V. Tadevosyan, J. Taylor, R. L. Trotta, A. Usman, C. Yero, M. Yurov, S. Zhamkochyan, S. A. Wood, & J. Zhang. (2025). The SHMS 11 GeV/c Spectrometer in Hall C at Jefferson Lab.